Ba_2LnSbO_6 and Sr_2LnSbO_6 (Ln = Dy, Ho, Gd) double perovskites: Lanthanides in the geometrically frustrating fcc lattice

H. Karunadasa*, Q. Huang†, B. G. Ueland‡, P. Schiffer‡, and R. J. Cava*§¶

*Department of Chemistry, Princeton University, Princeton, NJ 08544; †Center for Neutron Research, National Institute of Standards and Technology, Gaithersburg, MD 20899; ‡Department of Physics and Materials Research Institute, Pennsylvania State University, University Park, PA 16802; and §Princeton Materials Institute, Princeton University, Princeton, NJ 08540

This contribution is part of the special series of Inaugural Articles by members of the National Academy of Sciences elected on May 1, 2001.

Contributed by R. J. Cava, April 21, 2003

Magnetic ground states in solids often arise as a result of a delicate balance between competing factors. One currently active area of research in magnetic materials involves compounds in which long-range magnetic ordering at low temperatures is frustrated by the geometry of the crystalline lattice, a situation known as geometrical magnetic frustration. The number of systems known to display the effects of such frustration is growing, but those that are sufficiently simple from theoretical, chemical, and physical perspectives to allow for detailed understanding remain very few. A search for model compounds in this family has led us to the double perovskites Ba_2LnSbO_6 and Sr_2LnSbO_6 (Ln = Dy, Ho, and Gd) reported here. Ba_2DySbO_6, Ba_2HoSbO_6, Sr_2DySbO_6, and Sr_2HoSbO_6 are structurally characterized by powder neutron diffraction at ambient temperature. The trivalent lanthanides and pentavalent antimony are found to be fully ordered in the double-perovskite arrangement of alternating octahedra sharing corner oxygens. In such a structure, the lanthanide sublattice displays a classical fcc arrangement, an edge-shared network of tetrahedra known to result in geometric magnetic frustration. No magnetic ordering is observed in any of these compounds down to temperatures of 2 K, and in the case of the Dy-based compounds in particular, frustration of the magnetic ordering is clearly present. Lanthanide-based double perovskites are proposed to be excellent model systems for the detailed study of geometric magnetic frustration.

Despite decades of intensive investigation of the properties of magnetic materials, relatively little is known about compounds for which the long-range magnetic ordering of strongly interacting spins at low temperatures is frustrated by their geometric arrangement in the crystal lattice. The geometries of such frustrating lattices typically are based on corner-sharing triangles. This geometry makes long-range spin ordering that strictly satisfies near-neighbor pairwise antiferromagnetic interactions impossible. The resulting compromises in the spin orientations at low temperatures result in the existence of many energetically equivalent magnetic ground states (see refs. 1–4 for a review of the field). The 2D Kagomé lattice (named after a form of Japanese basket weaving) of corner-shared triangles of magnetic ions and its 3D extension to yield a corner-shared arrangement of magnetic tetrahedra (shown in Fig. 1) are of greatest current interest. Good examples of 2D Kagomé lattice magnetic compounds are found among the Jarosites (5, 6). The frustrating properties of the corner-sharing tetrahedron lattice have been particularly well studied for the magnetic lanthanide pyrochlores. Phenomena such as the formation of "spin ice" in $Ho_2Ti_2O_7$ and $Dy_2Ti_2O_7$ (7–11), the magnetic analogy of the geometric frustration of the ordering of hydrogen in ice at low temperatures, and the complex applied field/temperature magnetic-phase diagram in $Gd_2Ti_2O_7$ (12) are examples of the consequences of geometric frustration in the corner-shared tetrahedron lattice.

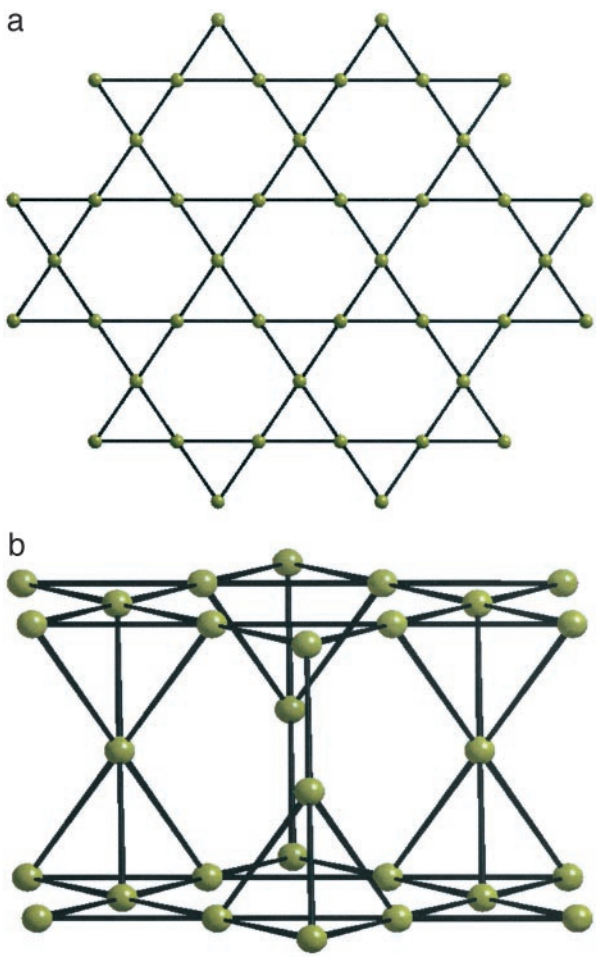

Fig. 1. Comparison of geometrically frustrating lattices based on corner-sharing triangles. (*a*) The 2D Kagome lattice. (*b*) The 3D pyrochlore lattice.

The lanthanide ions Ho, Dy, and Gd have been of particular interest in the pyrochlores because of the detailed character of their spin–spin interactions, the former often being Ising-like, and Gd displaying an isotropic spin. The work reported here is directed at finding compounds of those elements in different frustrating geometries than have been previously studied. The perovskite structure, formula ABO_3, is ubiquitous in oxide chemistry. It consists of a 3D lattice of fully corner-sharing BO_6 octahedra enclosing a cavity in which the larger atom (A) is

¶To whom correspondence should be addressed. E-mail: rcava@princeton.edu.

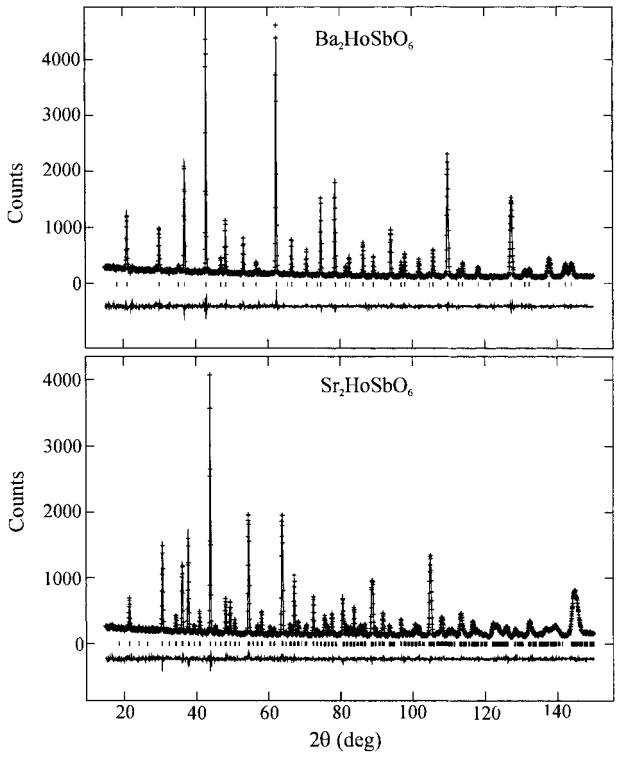

Fig. 2. Ambient temperature powder neutron diffraction data for Ba_2HoSbO_6 (*Upper*) and Sr_2HoSbO_6 (*Lower*). Crosses are raw data, and solid line indicates fit. Vertical lines indicate calculated peak positions. Shown below is the difference between observed and calculated intensities.

12-coordinated to oxygen. Many variants are known. The double perovskites, formula $A_2BB'O_6$, have chemical supercells in which two kinds of ions are found in the B sites in alternating octahedra. Perfectly ordered double perovskites, with only one of the two B-site ions carrying spin, have magnetic sublattices consisting of edge-shared tetrahedra (see Fig. 4*a*), another frustrating geometry in three dimensions. This edge-sharing geometry is the classical fcc lattice. Double perovskites in which magnetic transition elements occupy half of the B sites in an ordered manner have been studied (1), and recently a spin ½ transition metal variant Sr_2CaReO_6 has been characterized (13).

Table 1. Structural parameters and selected interatomic distances (Å) and angles (degrees) for Ba_2LnSbO_6 (*Ln* = Ho, Dy) at room temperature

	(*RE*)	Ho	Dy
	a (Å)	8.4119 (1)	8.4247 (1)
Ba	B (Å²)	0.63 (2)	0.67 (3)
Ln	B (Å²)	0.22 (2)	0.48 (2)
Sb	B (Å²)	0.38 (4)	0.41 (5)
O	*x*	0.26410 (9)	0.2646 (2)
	B_{11} (Å²)	0.47 (3)	0.38 (6)
	$B_{22} = B_{33}$ (Å²)	1.19 (2)	1.44 (3)
	R_p (%)	4.57	4.88
	R_{wp} (%)	5.71	5.93
	χ^2	1.09	0.91
Ba-O	×12	2.9764 (4)	2.9810 (8)
Ln-O	×6	2.2216 (7)	2.229 (2)
Sb-O	×6	1.9844 (7)	1.984 (2)

Space group $Fm\bar{3}m$. Atomic positions: Ba: 8*c* (¼, ¼, ¼); *Ln*: 4*a* (0 0 0); Sb: 4*b* (½, ½, ½); O: 24*e* (*x* 0 0).

Here we report the existence, structure, and preliminary magnetic characterization of the Ho-, Dy-, and Gd-based double perovskites Ba_2LnSbO_6 and Sr_2LnSbO_6. These compounds, with edge-shared tetrahedra of magnetic lanthanides, are of particular interest for direct comparison of their magnetic properties to those of the equivalent lanthanide pyrochlores, where the magnetic lattice consists of corner-sharing tetrahedra. The Ho-, Dy-, and Gd–based double perovskites show the characteristics of geometric magnetic frustration, and further characterization of their properties at temperatures <2 K will be of considerable interest. Double perovskites of the same type are expected to exist over the whole lanthanide series. Our results suggest that

Table 2. Structural parameters and selected interatomic distances (Å) and angles (degrees) for Sr_2LnSbO_6 (*Ln* = Ho, Dy) at room temperature

		Ho	Dy
	a (Å)	5.8141 (2)	5.8224 (2)
	b (Å)	5.8400 (2)	5.8538 (2)
	c (Å)	8.2361 (3)	8.2507 (3)
	β (°)	90.162 (2)	90.186 (2)
Sr	*x*	0.0074 (5)	0.0059 (9)
	y	0.0281 (2)	0.0291 (4)
	z	0.2505 (5)	0.2496 (7)
	B (Å²)	0.83 (2)	0.78 (2)
Ln	B (Å²)	0.25 (4)	0.29 (2)
Sb	*B* (Å²)	0.39 (5)	0.34 (4)
O(1)	*x*	0.2690 (5)	0.2692 (8)
	y	0.2970 (5)	0.2992 (8)
	z	0.0374 (4)	0.0391 (7)
	B (Å²)	1.02 (6)	0.82 (7)
O(2)	*x*	0.3019 (3)	0.3029 (9)
	y	0.2737 (5)	0.2735 (9)
	z	0.4605 (4)	0.4621 (6)
	B (Å²)	0.83 (5)	0.83 (7)
O(3)	*x*	−0.0724 (4)	−0.0738 (8)
	Y	0.4820 (4)	0.4778 (7)
	Z	0.2351 (4)	0.2347 (6)
	B (Å²)	0.79 (3)	0.81 (6)
	R_p (%)	4.24	4.06
	R_{wp} (%)	5.18	4.94
	χ^2	1.016	0.89
Sr-O(1)		2.807 (5)	2.807 (9)
Sr-O(1)		2.559 (5)	2.560 (7)
Sr-O(1)		3.433 (5)	3.451 (7)
Sr-O(1)		2.927 (5)	2.939 (9)
Sr-O(2)		2.822 (4)	2.845 (7)
Sr-O(2)		2.543 (4)	2.558 (7)
Sr-O(2)		3.468 (5)	3.472 (8)
Sr-O(2)		2.908 (5)	2.888 (8)
Sr-O(3)		3.225 (2)	3.262 (4)
Sr-O(3)		2.694 (3)	2.670 (4)
Sr-O(3)		2.546 (4)	2.538 (6)
Sr-O(3)		3.298 (4)	3.322 (6)
Ln-O(1)	×2	2.216 (3)	2.232 (4)
Ln-O(2)	×2	2.222 (3)	2.229 (5)
Ln-O(3)	×2	2.224 (3)	2.233 (5)
Sb-O(1)	×2	1.986 (3)	1.985 (4)
Sb-O(2)	×2	1.996 (3)	1.994 (5)
Sb-O(3)	×2	1.985 (3)	1.989 (5)
Ln-O(1)-Sb		157.4 (2)	156.5 (3)
Ln-O(2)-Sb		155.3 (2)	155.6 (3)
Ln-O(3)-Sb		156.1 (1)	155.4 (2)

Space group $P2_1/n$. Atomic positions: Sr: 4e (*x y z*); *Ln*: 2*d* (½, 0, 0); Sb: 2*c* (0, ½, 0); O(1): 4*e* (*x y z*); O(2): 4*e* (*x y z*); O(3): 4*e* (*x y z*).

these lanthanide-based double perovskites are an excellent prototype family for making contact with theoretical models for the behavior of spins of different types on the fcc lattice. The lanthanide ions vary in total spin and electron configuration in a systematic manner that is not observed for transition metals (because of the complexities of d-electron interactions) where the fcc structure is very commonly observed, and therefore fcc lanthanide lattices offer a unique opportunity for detailed comparison to theoretical models.

Experiments

Two-gram samples of the Gd, Dy, and Ho analogs of Sr_2LnSbO_6 and Ba_2LnSbO_6 were prepared from the high-purity starting materials $SrCO_3$, $BaCO_3$, Gd_2O_3, Dy_2O_3, Ho_2O_3, and Sb_2O_5. Stoichiometric mixtures of these powders were mixed in an agate mortar and heated in air in dense, high-purity Al_2O_3 crucibles. Samples were heated at 1,400°C for a total of 48 h with several intermediate grindings and were observed to be single phase by powder x-ray diffraction (Cu Kα radiation) before study by neutron diffraction or magnetic susceptibility measurements.

Magnetic susceptibilities were measured between 2 and 320 K in an applied field of 200 Oe in a SQUID magnetometer (Quantum Design, San Diego). The crystal structures of the Dy- and Ho-based compounds were determined at ambient temperature by powder neutron diffraction, at the National Institute of Standards and Technology Center for Neutron Research, on the high-resolution powder neutron diffractometer with monochromatic neutrons of wavelength 1.5402 Å produced by a Cu(311) monochromator. (The Gd-based compounds were studied by susceptibility only, because of the strong neutron absorption of Gd.) Data were collected at ambient temperature between 3° and 168° diffraction angles with a step size of 0.05°. Collimators with horizontal divergences of 15′, 20′, and 7′ of arc were used before and after the monochromator, and after the sample, respectively. Structure refinement by the Rietveld method was carried out with the program GSAS (14). The neutron scattering amplitudes used in the refinement were 0.525, 0.702, 1.69, 0.808, 0.564, and 0.581 ($\times 10^{-12}$ cm) for Ba, Sr, Dy, Ho, Sb, and O, respectively (14). Statistical uncertainties quoted in all of the neutron results represent one standard deviation.

Results

The ambient temperature powder neutron diffraction patterns for the Ba_2HoSbO_6 and Sr_2HoSbO_6 double perovskites are presented in Fig. 2. The data from the Dy analogs are very highly analogous. Qualitative inspection of the patterns shows that the Sr variant has lower symmetry than the Ba variant. Both patterns can be indexed by crystallographic cells that are commonly found for double perovskites. The Ba variants can be best described by the high-symmetry cubic doubled perovskite cell, space group $Fm\bar{3}m$, with cell parameters (Å): a = 8.4119(1) and a = 8.4247(1) for Ho and Dy, respectively. The Sr variants can best be described by a monoclinic symmetry cell, space group $P2_1/n$. The cell parameters are: (Å) a = 5.8141(2), b = 5.8400(2), c = 8.2361(3), β = 90.162(2)° for Ho, and a = 5.8224(2), b = 5.8538(2), c = 8.2507(3), β = 90.186(2)° for Dy. The latter cells are very similar to those recently reported for the equivalent lanthanides in the Sr_2LnTaO_6 and Sr_2LnIrO_6 double perovskite families (15, 16). The Ba_2LnNbO_6 family is also apparently monoclinic (17).

The structural refinements indicate that the compounds display classic double-perovskite structures. As observed previously in other lanthanide-containing double perovskites (15–17), the present compounds show full ordering of the Ln^{3+} B-site ion and the nonmagnetic 5+ B-site ion, in this case Sb, in the available B sites, with the perfect ordering likely driven by differences in both charge and size. This is very important from the magnetic point of view, as disorder among the magnetic atoms significantly disrupts the geometrical frustration (1, 18). There are only minor differences in the structures for the two lanthanides in the current compounds, attributable to the slight difference in size between Ho and Dy. The structural parameters, bond lengths, and refinement particulars are summarized in Tables 1 and 2. The crystal structures are presented in Fig. 3. Fig. 3 shows that the reduced symmetry of the Sr variants is caused by the relatively smaller size of the Sr on the A site, resulting in the

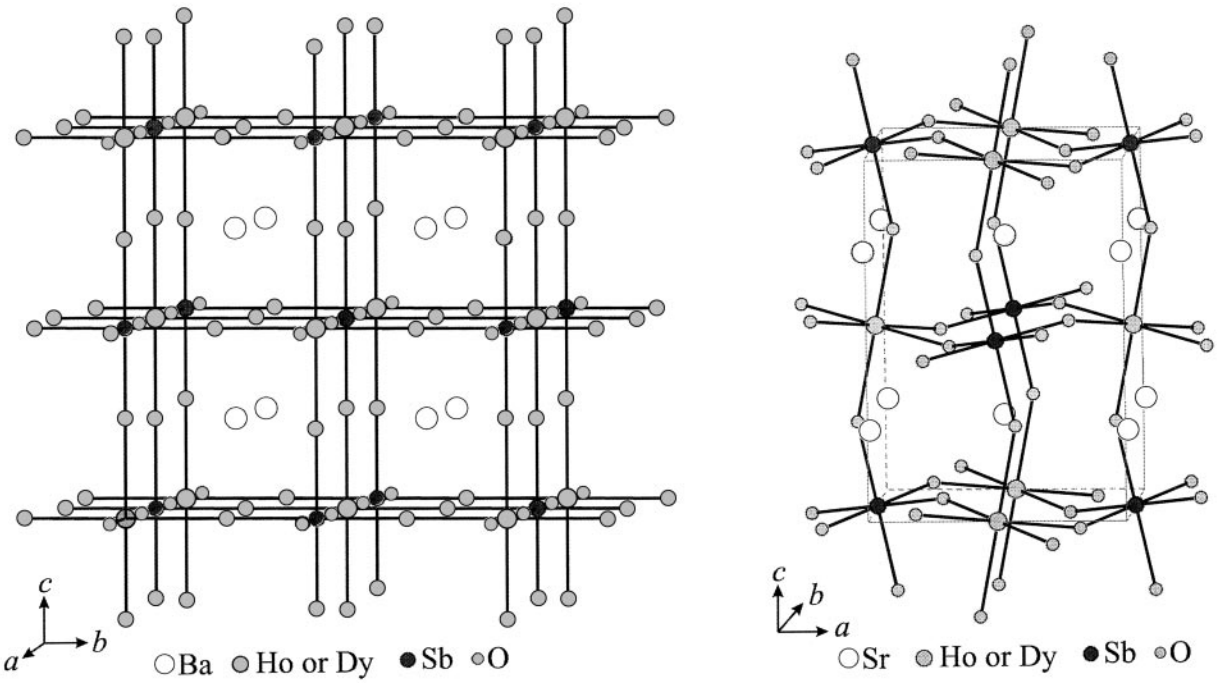

Fig. 3. The crystal structures of Ba_2LnSbO_6 (*Left*) and Sr_2LnSbO_6 (*Right*). Atom types are as marked. Unit cell and B-site octahedra are outlined.

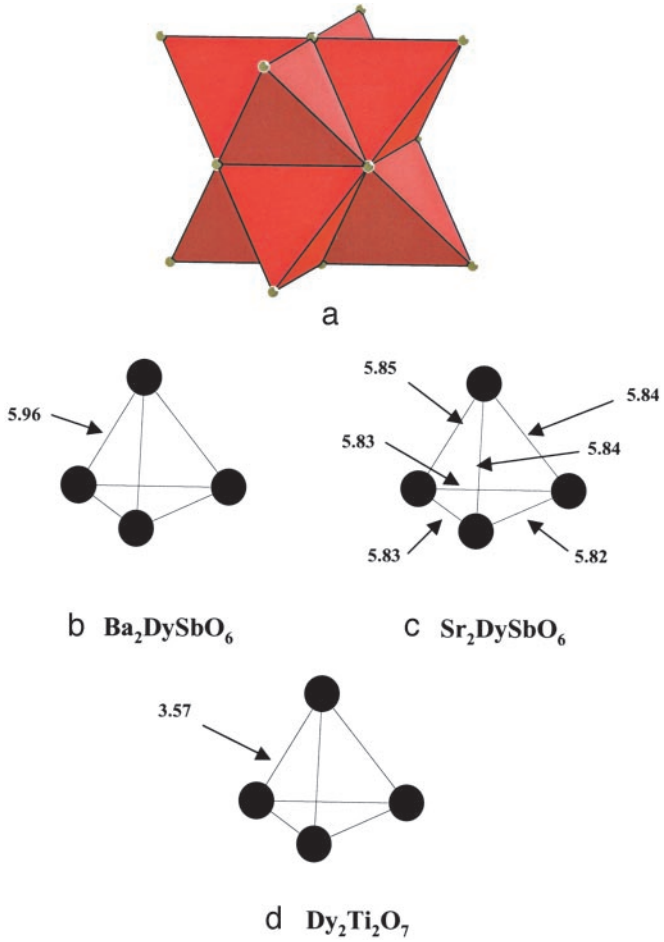

Fig. 4. The magnetic sublattice in the lanthanide double perovskites. Only magnetic lanthanide atoms are shown. (*a*) The arrangement of edge-shared magnetic atom tetrahedra in double perovskites. (*b*) The magnetic atom tetrahedron in Ba_2DySbO_6. (*c*) The magnetic atom tetrahedron in Sr_2DySbO_6. (*d*) The magnetic atom tetrahedron in $Dy_2Ti_2O_7$ for comparison. All distances are in Å.

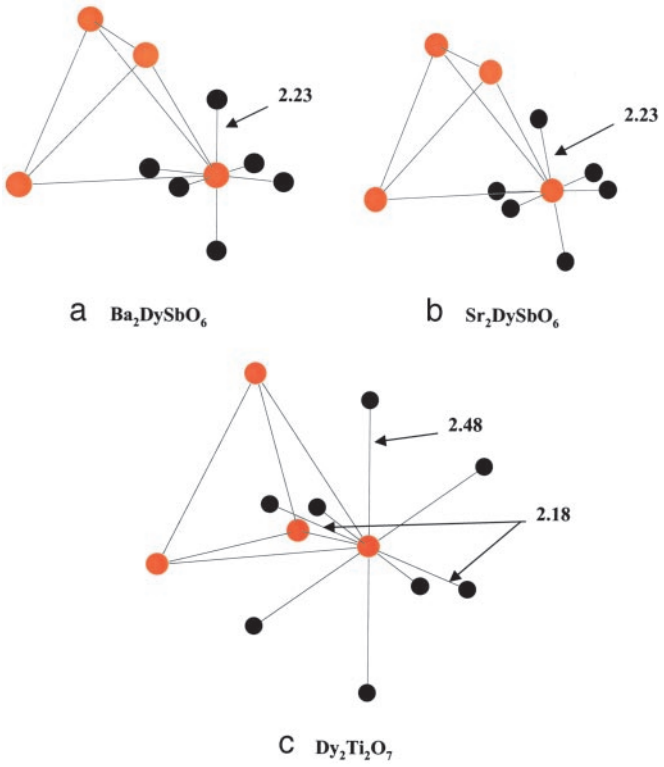

Fig. 5. The Ln-O coordination polyhedra and their relationship to the Ln tetrahedra in Sr_2DySbO_6 (*a*), Ba_2LnSbO_6 (*b*), and Dy_2Ti2O_7 (*c*). Large colored circles indicate Dy, and small black circles indicate oxygen.

frequently observed partial collapse of the ideal perovskite cavity through rotations of the BO_6 octahedra about their shared corners, allowing for the appropriate Sr—O bond lengths.

Fig. 4 shows the characteristics of the magnetic sublattices for the Dy and Ho double perovskites and compares them to that of the pyrochlore. Only the magnetic lanthanides are shown in Fig. 4*a*, which clarifies the arrangement of the edge-shared tetrahedra of magnetic ions found in the double perovskites. The fcc character of this arrangement is apparent. Fig. 4 *b* and *c* extracts individual magnetic ion tetrahedra from Ba_2DySbO_6 and Sr_2DySbO_6. In both compounds, only one type of magnetic tetrahedron is present. In the Ba compound, the tetrahedron is dimensionally regular, with a Dy–Dy separation of 5.96 Å. In the Sr compound, the Dy–Dy distances are somewhat shorter, ≈5.85 Å, and there is a range of separations of ≈0.03 Å, which is not substantial. Thus the magnetic tetrahedra are only slightly different in size and shape in the two kinds of compounds. Comparison to the size of the Dy tetrahedron in the $Dy_2Ti_2O_7$ pyrochlore is made in Fig. 4*d*. It is seen that the tetrahedra are quite different in size in the pyrochlore and double-perovskite structures, expected to significantly affect the relative strength of the magnetic coupling.

The local coordination polyhedron of oxygen around the lanthanides in the double-perovskite and pyrochlore structures is quite different. A comparison of the shapes and sizes of the local lanthanide coordination polyhedra for the Dy double perovskites and the Dy pyrochlore is presented in Fig. 5. In the pyrochlore, the local Ln site symmetry is $\bar{3}m$, and there are six near-neighbor oxygens, two of which are substantially closer to the Dy than the other four (Fig. 5*c*). In the perovskites, the local lanthanide symmetry is $m\bar{3}m$ in the cubic Ba variants, with six oxygen near-neighbors in an ideal octahedral geometry (Fig. 5*b*) and $\bar{1}$ in the case of the monoclinic Sr variants, again with six oxygen neighbors, in a slightly distorted octahedral geometry. Fig. 5 shows that for the pyrochlores, very short Dy—O bond distances are found directly to an oxygen at the center of the magnetic tetrahedron, and to an equivalent oxygen in the directly opposite direction (⟨111⟩ directions). These correspond exactly to the directions that the Ising-like Dy spins take in that compound, showing the structural origin of the strong crystal field (19) that determines the preferred orientations of the spins. For the double perovskites, on the other hand, the situation is quite different. For the Ba variant, six exactly equivalent lanthanide-oxygen bonds are pointed along cubic ⟨100⟩ directions, and not into the magnetic tetrahedra. The same is generally true in the Sr variants, except that the six lanthanide-oxygen bonds are not exactly equivalent by symmetry, with the directions still generally along what are in that case the pseudocubic ⟨100⟩ directions. The regular character of the Ln—O octahedra in the double perovskites suggests that the crystal field will not be axial in these compounds, as it is in the pyrochlore case. Fig. 5 also shows that the orientations of the LnO_6 local coordination octahedra with respect to the magnetic tetrahedra are slightly different in the two types of double perovskites. These differences in local coordination vs. magnetic geometry may lead to differences in magnetic behavior at low temperatures.

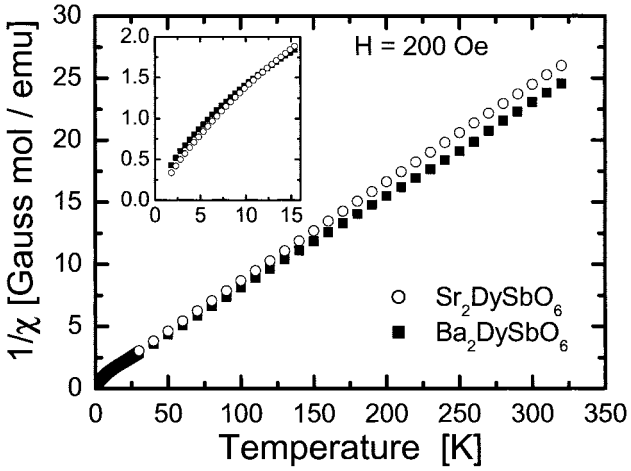

Fig. 6. Temperature dependence of the inverse magnetic susceptibilities for Ba_2DySbO_6 and Sr_2DySbO_6. (*Inset*) Detail of the low-temperature region.

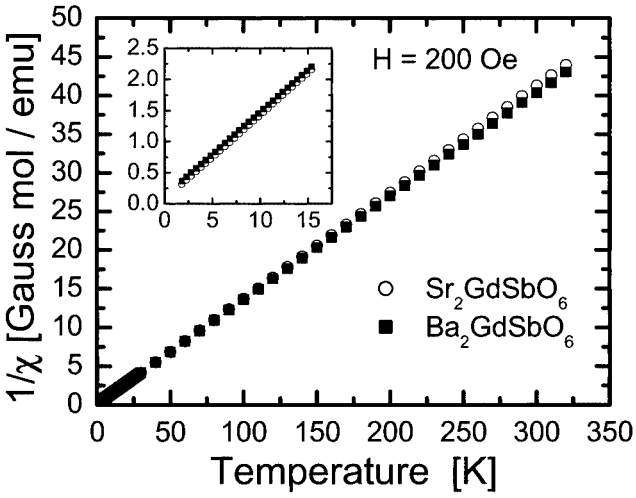

Fig. 8. Temperature dependence of the inverse magnetic susceptibilities for Ba_2GdSbO_6 and Sr_2GdSbO_6. (*Inset*) Detail of the low-temperature region.

The temperature-dependent magnetic susceptibility data for the six double perovskites studied are shown in Figs. 6–8. No magnetic transitions are observed down to a temperature of 2 K, and the Ba and Sr variants with the same lanthanide do not show substantially different behavior. The data are well described by the Curie–Weiss law at high temperatures, $\chi = C/(T - \theta_W)$, where the Curie constant C is proportional to the square of the effective magnetic moment and the Weiss temperature θ_W is a measure of the strength and type of near-neighbor magnetic interaction. Deviations from this behavior occur only at low temperatures (Figs. 6–8 *Insets*). The parameters for the fits are presented in Table 3, as are comparisons to the expected moments (20) for the lanthanides. The θ_Ws are all negative for the double perovskites, indicating the presence of antiferromagnetic nearest neighbor spin–spin interactions. In addition, the θ_W values for the Dy and Ho analogs for the high temperature fits (≈ -8 and -5 K, respectively) are comparable to those found in the pyrochlores, despite the substantially larger Ln–Ln spacing in the perovskites. (The lower temperature portions of the susceptibility curves have also been fit to the Curie–Weiss law, with the parameters shown in Table 3, to facilitate comparison to the pyrochlores where this temperature region is sometimes quoted in the characterizations.) Figs. 6–8 *Insets* show an interesting difference between the lowest temperature behaviors of the Dy- and Ho-based compounds. The Ho susceptibilities deviate toward lower values at the lowest temperatures measured, suggesting increasing antiferromagnetic correlations and perhaps incipient long-range order. The Dy susceptibilities, on the other hand, deviate toward higher values at lower temperatures, suggesting increasing ferromagnetic correlations or the presence of a small paramagnetic component to the susceptibility, as has been observed in other geometrically frustrated magnets (21, 22). The Gd-based materials, on the other hand, maintain their strict Curie–Weiss behavior to the lowest temperatures studied, with the Curie–Weiss θ values relatively quite small, on the order of 1 K.

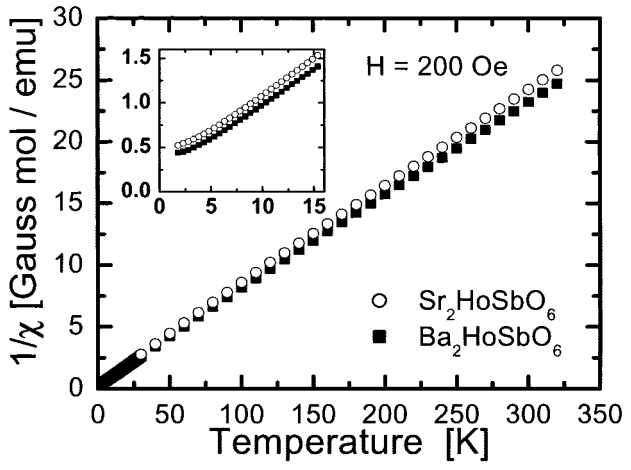

Fig. 7. Temperature dependence of the inverse magnetic susceptibilities for Ba_2HoSbO_6 and Sr_2HoSbO_6. (*Inset*) Detail of the low-temperature region.

The expected magnetic ordering behavior for antiferromagnetically interacting Heisenberg spins on an fcc lattice has been modeled and simulated theoretically (23). For such a system, the magnetic ordering is expected at a temperature of 0.45 J, where J is the strength of the nearest neighbor coupling. For fcc lattices, the geometry dictates that the measured θ_W in the Curie–Weiss fit is 4 J. Thus theory predicts an antiferromagnetic long-range ordering temperature (T_N) of $T_N/\theta_W = 8$ as a result of the frustrating geometry of the fcc lattice. [In the mean field picture in nonfrustrating lattices, ordering is expected for $T_N/\theta_W = 1$–2 (1).] Interactions between spins on the fcc lattice beyond nearest neighbor coupling will increase T_N toward θ_W. For the fcc Dy, Ho, and Gd lattices in the current materials, where no magnetic ordering is observed down to 2 K, only the Dy case can be considered to be clearly showing the effects of geometric frustration, as T_N/θ_W must be >4. Sub-2 K measurements will be required to clarify the behavior of all of these compounds.

Conclusions

Double perovskites with lanthanides ordered on one subset of the octahedrally coordinated B sites have recently been of crystal chemical interest (13–16). In the present work we have described a few members of a family of such double perovskites, with Ln^{3+}–Sb^{5+} ordering on the B sites. The antiferromagnetic near-neighbor coupling found for the Ho- and Dy-based double perovskites is different from the spin-ice pyrochlores based on those elements, where the nearest-neighbor coupling is ferromagnetic. Critical to the observation of the spin ice behavior in the Dy and Ho pyrochlores is the presence of significant magnetocrystalline anisotropy. The spins are Ising-like, with preferred directions toward or away from the centers of the magnetic tetrahedra, the ⟨111⟩ orientations. It is not known at

Table 3. Effective moments (p), Weiss temperatures (θ_W), and goodness of fit (R^2) determined by least-squares fitting of the Curie–Weiss law to the magnetic susceptibility data in Figs. 5–7

Compound	p (high T)	θ_W (high T)	R^2 of fit	p (low T)	θ_W (low T)	R^2 of fit	p_{exp}
Ba_2DySbO_6	10.37 (2)	−8.6 (3)	0.99994	10.55 (5)	−10.06 (8)	0.99948	10.6
Sr_2DySbO_6	10.01 (1)	−8.2 (3)	0.99997	9.82 (3)	−7.15 (8)	0.9987	10.6
Ba_2HoSbO_6	10.20 (1)	−4.7 (2)	0.99976	9.93 (2)	−2.00 (3)	0.99999	10.4
Sr_2HoSbO_6	9.99 (1)	−5.5 (2)	0.99970	9.73 (2)	−2.79 (7)	0.99999	10.4
Ba_2GdSbO_6	7.72 (1)	−1.2 (2)	1	7.70 (2)	−0.95 (7)	1	8.0
Sr_2GdSbO_6	7.64 (1)	−0.1 (4)	0.99990	7.67 (2)	−0.46 (9)	1	8.0

Temperature range of fits: high T, 30–320 K, data temperature interval 10 K; low T, 10.36–30 K. Expected moment (p_{exp}) from ref. 20.

this time how the lanthanide spins interact in the double perovskites, but both the crystal fields and their orientations with respect to the magnetic tetrahedra are different from those in the pyrochlores. If the preferred spin directions are along ⟨100⟩, a 6-fold degeneracy results, which, combined with the edge-sharing geometry in the double perovskites, makes the Dy and Ho double perovskites distinctly different from the equivalent pyrochlores. Detailed study of the magnetic properties of these and additional fcc lanthanide double perovskites at temperatures <2 K will be of significant interest.

This work was partially supported by National Science Foundation Grant DMR 9725979 and Army Research Office Presidential Early Career Awards for Scientists and Engineers Grant DAAD19-01-1-0021.

1. Ramirez, A. P. (1994) *Annu. Rev. Mater. Sci.* **24,** 453–480.
2. Greedan, J. E. (2001) *J. Mater. Chem.* **11,** 37–53.
3. Moessner, R. (2001) *Can. J. Phys.* **79,** 1283–1294.
4. Schiffer, P. & Ramirez, A. P. (1996) *Comments Condens. Matter Phys.* **18,** 21–50.
5. Papoutsakis, D., Grohol, D. & Nocera, D. G. (2002) *J. Am. Chem. Soc.* **124,** 2647–2656.
6. Willis, A. S. & Harrison, A. J. (1996) *J. Chem. Soc. Faraday Trans.* **92,** 2161–2166.
7. Harris, M. J., Bramwell, S. T., McMorrow, D. F., Zeiske, T. & Godfrey, K. W. (1997) *Phys. Rev. Lett.* **79,** 2554–2557.
8. Harris, M. J., Bramwell, S. T., Holdsworth, P. C. W. & Champion, J. D. M. (1998) *Phys. Rev. Lett.* **81,** 4496–4499.
9. Bramwell, S. T. & Harris, M. J. (1998) *J. Phys. Condens. Matter* **10,** L215–L220.
10. Ramirez, A. P., Hayashi, A., Cava, R. J., Siddharthan, R. & Shastry, B. S. (1999) *Nature* **399,** 333–335.
11. Harris, M. J. (1999) *Nature* **399,** 311–312.
12. Ramirez, A. P., Shastry, B. S., Hayashi, A., Krajewski, J. J., Huse, D. A. & Cava, R. J. (2002) *Phys. Rev. Lett.* **89,** 067202.
13. Wiebe, C. R., Greedan, J. E., Luke, G. M. & Gardner, J. S. (2002) *Phys. Rev. B Condens. Matter* **65,** 144413.
14. Larson, A. & Von Dreele, R. B. (1994) *Los Alamos National Laboratory Internal Report* (Los Alamos National Laboratory, Los Alamos, CA).
15. Hirada, D., Wakashima, M. & Hinatsu, Y. (1999) *J. Solid State Chem.* **145,** 356–360.
16. Kanaiwa, Y., Wakashima, M. & Hinatsu, Y. (2002) *Mater. Res. Bull.* **37,** 1825–1836.
17. Henmi, K., Hinatsu, Y. & Masaki, N. M. (1999) *J. Solid State Chem.* **148,** 353–360.
18. Snyder, J., Slusky, J. S., Cava, R. J. & Schiffer, P. (2002) *Phys. Rev. B Condens. Matter* **66,** 064432.
19. Rosenkranz, S., Ramirez, A. P., Hayashi, A., Cava, R. J., Siddharthan, R. & Shastry, B. B. (2000) *J. Appl. Phys.*, **87,** 5914–5916.
20. Kittel, C. (1992) *Introduction to Solid State Physics* (Wiley, New York), p. 425.
21. Schiffer, P. & Daruka, I. (1997) *Phys. Rev. B Condens. Matter* **56,** 13712–13715.
22. Moessner, R. & Berlinsky, A. J. (1999) *Phys. Rev. Lett.* **83,** 3293–3296.
23. Diep, H. T. & Kawamura, H. (1989) *Phys. Rev. B Condens. Matter* **40,** 7019–7022.